# CARMENES. III: an innovative and challenging cooling system for an ultra-stable NIR spectrograph

S. Becerril*[a], J.L. Lizon[b], M.A. Sánchez-Carrasco[a], E. Mirabet[a, b], P. Amado[a], W. Seifert[c], A. Quirrenbach[c], H. Mandel[c], J.A. Caballero[d], I. Ribas[e], A. Reiners[f], M. Abril[a], R. Antona[a], C. Cárdenas[a], R. Morales[a], D. Pérez[a], A. Ramón[a], E. Rodríguez[a], J. Herranz[g]

[a] Instituto de Astrofísica de Andalucía (CSIC), Glorieta de la Astronomía s/n, E-18008 Granada, Spain.
[b] European Southern Observatory, Karl-Schwarzschilds-Str., Garching bei München D-85748, Germany.
[c] Landessternwarte, ZAH, Königstuhl 12, D-69117 Heidelberg, Germany.
[d] Centro de Astrobiología (CSIC-INTA), Carretera de Ajalvir km 4, E-28850 Torrejón de Ardoz, Madrid, Spain.
[e] Institut de Ciències de l'Espai (CSIC-IEEC), Facultat Ciències, Torre C5, E-08193 Bellaterra, Barcelona, Spain.
[f] Institut für Astrophysik (GAU), Friedrich-Hund-Platz 1, D-37077 Göttingen, Germany.
[g] Proactive Research & Development, S.L.

## ABSTRACT

The CARMENES project, which is currently at FDR stage, is a last-generation exoplanet hunter instrument to be installed in the Calar Alto Observatory by 2014. It is split into two different spectrographs: one works within the visual range while the other does it in the NIR range. Both channels need to be extremely stable in terms of mechanical and thermal behavior. Nevertheless, due to the operation temperature of the NIR spectrograph, the thermal stability requirement ($\pm0.07$ K in 24 hours; $\pm0.01$ K (goal)) becomes actually a major challenge. The solution here proposed consists of a system that actively cools a shield enveloping the optical bench. Thus, the instability produced on the shield temperature is further damped on the optical bench due to the high mass of the latter, as well as the high thermal decoupling between both components, the main heat exchange being produced by radiation.

This system -which is being developed with the active collaboration and advice of ESO (Jean-Louis Lizon)- is composed by a previous unit which produces a stable flow of nitrogen gas. The flow so produced goes into the in-vacuum circuitry of the NIR spectrograph and removes the radiative heat load incoming to the radiation shield by means of a group of properly dimensioned heat exchangers.

The present paper describes and summarizes the cooling system designed for CARMENES NIR as well as the analyses implemented.

**Keywords:** Cooling, stability, thermal performance, cryogenics, large instrument, extrasolar planets, near-infrared instrumentation

## 1. INTRODUCTION

The CARMENES project is presently at final design phase. One of the key systems to ensure the good performance of the NIR spectrograph is the cooling system, which was already the subject of a paper presented at SPIE 2010**. The progress implemented on this system is here described.

*Contact Santiago Becerril (santiago@iaa.es) for further information.

**Becerril, S., "Comprehensive transient-state study for CARMENES NIR high-thermal stability", Proc. SPIE 7735, 77352S-1 to 77352S-13 (2010)

The project successfully passed the PDR review in July 2011, where several options about the cooling system were presented, only one of them being selected to be developed further at final design phase. The system here developed is based on the CFC system (Continuous Flow Cooling) which has been extensively tested and implemented in instruments built by ESO (European Southern Observatory). Further detail is given on the description of this system in section 3. Nevertheless, the main innovation here consists of the adaptation of the CFC system for thermal stabilization in large instruments in the range of centikelvin.

The main issue in terms of thermal performance lies on the temperature stability requirement (see section 2). Therefore, the present work includes the analyses carried out to know the steady-state temperature distribution as well as the thermal stability under a sine-shaped input signal.

## 2. REQUIREMENTS OF THE COOLING SYSTEM

The main thermal requirements of the instrument are listed in Table 1, the most challenging one being the thermal stability. At present, there is not a requirement on the temperature gradient; however, this issue has been taken into account in the analyses here detailed (see section 4) because large, deep gradients on the temperature distribution across the instrument would become a source of instability.

Concerning the working temperature requirement, note that the final absolute value of such a figure is not critical; in other words, once the desired temperature is achieved within few tenths of Kelvin, the critical issue consists of keeping such temperature conditions according to the temperature stability requirement. Therefore, smooth gradients are an important issue since they ensure that no part of the spectrograph is above an excessive temperature which may deliver a too large thermal background into the detector, hence degrading the SNR performance of the instrument.

Table 1. Thermal requirements applicable

| Requirement | Value |
|---|---|
| Working temperature | ~140 K |
| Temperature stability | ±0.07 K  (±0.01 K goal) in the timescale of 1 day |
| Pre-cooling time | 48h (goal) |
| Cooldown and warm-up rate for the optics | <10 K/h |
| Liquid nitrogen consumption | <90l/day |
| Environment temperature | 285±0.5 K |
| Vacuum level | ~$10^{-6}$mbar |

## 3. MAIN GUIDELINES OF THE COOLING SYSTEM

The guidelines driving the cooling system are mainly focused on the aim of providing the extremely high thermal stability required. Therefore, all the opto-mechanical systems will be supported on a single bench called optical bench. This way all the opto-mechanics will be similarly affected in terms of thermal stability. It means that the hardware needing thermal stability according to the requirement shown in Table 1 is only limited to the optical bench and the systems supported on there.

Radiation transfer has been prioritized for providing the required stability to the optical bench, which means that the latter is enclosed inside a radiation shield that is, in turn also cooled down to working temperature. With respect to other ways of heat transfer, convection is not applicable since the whole instrument must be in vacuum. On the other hand, conduction transfer, if displayed by means of heat exchangers directly attached to the optical bench, would imply noticeably deeper gradients since the heat exchange area would be very small as compared to the total area of the optical bench. Alternatively, conduction transfer might be done by means of a typical LN2-bath cryostat. Although this solution

would play on the high thermal stability of the liquid/gas phase change of nitrogen, there would be the following undesirable consequences:

- The size of the Vacuum Vessel would be noticeably enlarged due to the volume of the LN2 tank.

- Alternatively, the shape of the optical bench could be dramatically changed in order to compact the volume: It would be much more complex, an additional benefit in terms of dimensional stability being as well lost. Indeed, the current concept proposed for the optical bench is based on a very simple shape where sharp changes in shape are avoided. Thus, the differential behavior between different sections of the optical bench is likely to be similar in the event of stress relief during the lifetime of the instrument. This is not the case if the optical bench gets a complex shape. In addition to this guideline for the design of the optical bench, dimensional stability of the mechanical hardware involved will be ensured by providing a thermal treatment for stress relief and artificial ageing of the materials after manufacturing.

- The working temperature would be, in fact, much lower than required, which may introduce tighter requirements to the opto-mechanics.

Anyway, approaches based on heat conductive transfer to the optical bench for thermal stability purposes would also include the presence of a radiation shield cooled down to working temperature. That is why the radiative approach is here preferred as compared to the conductive approach. Furthermore, this way the cross-coupled view factors affecting the radiative exchange between the Radiation Shield and the optical bench will make the temperature distribution on the latter noticeably smoother than the one existing on the radiation shield.

Obviously, heat exchangers attached to the optical bench will be necessary for a fast cooling down from room temperature to working temperature. Meanwhile, also the radiation shield will be cooled down from room temperature but it will take not so long because its mass is much lower than the one of the optical bench. Once the temperature is under a certain value (140 K), the circuit feeding the heat exchangers on the optical bench is closed. At this point, only the circuit feeding the heat exchangers on the radiation shield keeps running whereas the temperature distribution on the optical bench is in a passive way being re-arranged until the steady-state is achieved. Once the temperature distribution on the optical bench is stable –within the requirement in Table 1- the instrument is ready for operation.

In a large instrument like CARMENES, the process above explained will take noticeably long. That is the reason why once the instrument starts operating, the temperature conditions will be kept continuously during the lifetime of the instrument except for major maintenance actions or incidents.

Since the thermal stability is achieved by radiation, the optical bench will be attached to the Vacuum Vessel but thermally decoupled from it. The same approach is applicable to the radiation shield. Of course, radiation shield and optical bench are thermally decoupled from each other.

At present, the cooling system of the CARMENES NIR channel is being designed in joint collaboration with ESO in order to properly adapt the CFC system, which has been extensively used and implemented in the instruments developed by ESO.


## 3.1 DESCRIPTION OF THE CFC SYSTEM

The CFC System is based on a series of cooling lines that dissipate the power from the radiation shield by means of a certain amount of heat exchangers (see Figure 2). The power to be dissipated comes mainly from the radiative exchange between the Vacuum Vessel and the radiation shield. In order to minimize that, the radiation shield is entirely covered by 20-layered MLI (Multi-Layer Insulation) (not shown in Figure 1).

The amount of heat exchangers connected in series in a cooling line has been limited to two units. Obviously, the first heat exchanger will be cooler than the second one, which means that a temperature gradient is produced by having both heat exchangers at a different temperature. Therefore, the higher the amount of heat exchangers connected in series is, the larger the temperature gradient induced. On the opposite case, all the cooling lines could include only one heat exchanger but the amount of cooling ports and hardware necessary makes this option quite unpractical.

The stability of the temperature distribution of the radiation shield depends on the stability of the radiative input from the Vacuum Vessel. Such input depends on the external conditions. Therefore, the instrument will be housed in a temperature-controlled room where the temperature will be stable within ±0.5 K.

On the other hand, the thermal stability on the radiation shield depends also on the stability of the conditions in which the coolant flow is delivered. For such purpose, a dedicated, independent unit has been designed by ESO. This unit is called Preparation Unit (see Figure 3 and Figure 4) and provides a fine control on the temperature and pressure of coolant flow exiting.

The Radiation shield is composed by a main body and two end covers. The main body includes 12 heat exchangers distributed into 6 cooling lines while each cover includes one heat exchanger. Therefore, the present design includes 8 cooling lines. Figure 1 shows a general view of the NIR spectrograph enclosed in the radiation shield envelope.
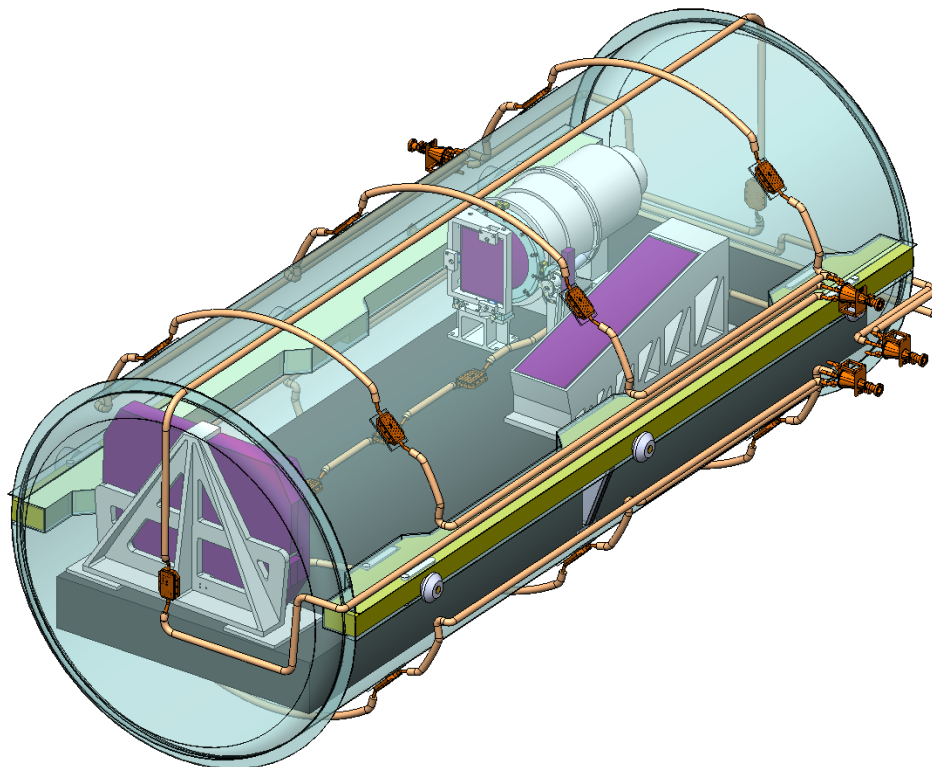


Figure 1. General view of the optical bench assembly -opto-mechanical systems are included- inside the radiation shield, as design for PDR. Note that the latter is displayed in transparent mode for better understanding of the view. Heat exchangers are also shown while the Vacuum Vessel is not.



Figure 2. General view of a heat exchanger developed by ESO and extensively used in their instrumentation.

### 3.1.1 The Preparation Unit

The CFC system is fed with LN2. Therefore, a new constraint is here applicable: facilities at Calar Alto include a LN2 production plant, which can produce as much as 150l per day. However, the CARMENES instrument shall coexist with the PANIC instrument, which consumes 35l per day, as well as other minor equipment. Additionally, the CARMENES NIR Detector Cryostat needs 2l per day. According to such scenario, the maximal daily consumption for CARMENES-NIR has been set to 90l of LN2 per day (see section 2).

The Preparation Unit consists of a vacuum tank where several systems are enclosed: the Evaporator Unit, the Intermediate Exchanger and the Final Heat Exchanger. All of them are equipped with heaters in order to supply the power required for the LN2 flow to reach the desired temperature. Once the LN2 comes into the Preparation Unit, the flow passes first through the Evaporator Unit. The power here supplied allows not only changing the phase of the flow from liquid to gas but also providing a temperature level close to the desired temperature. The Evaporator Unit includes different cross sections for the channel where nitrogen flows through. At the entrance to the Evaporator Unit, the cross section is small as compared to the cross section at the exit. Indeed, the liquid will expand into gas as it goes along the Evaporator Unit; so the expansion produced is, at a first level, accommodated in the last stage of this unit by means of the large cross-section channels.

The flow exiting the Evaporator Unit may not be very stable due to the turbulence produced in the phase change. At the exit from the Evaporator Unit, there is the Intermediate Exchanger, which consists of a long coil whose large cross section allows the flow getting even more stable in terms of pressure and temperature. This stage can be used to provide an additional temperature step to the flow.

After the Intermediate Exchanger, the flow comes into the Final Heat Exchanger. This stage provides a huge exchange area with the flow. Note that the incoming flow is close to the working conditions. Therefore, this big heat exchanger provides the last and small temperature step. Due to the high mass of the Final Heat Exchanger, the temperature reached by the flow will be very stable.

After the exit from the Final Heat Exchanger, the flow leaves the Preparation Unit and comes into the Vacuum Vessel. In order to minimize the losses in between, the pipe linking the Preparation Unit and the Vacuum Vessel must be vacuum insulated, its length being not more than 2m.

Note that the electrical hardware prone to maintenance (e.g. the heaters) are inside the Preparation Unit, the Vacuum Vessel being undisturbed if a heater needs to be replaced. Eventually, all the systems of the Preparation Unit are enclosed inside a radiation shield.
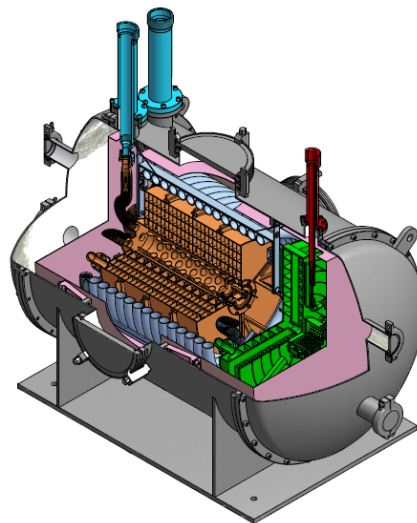


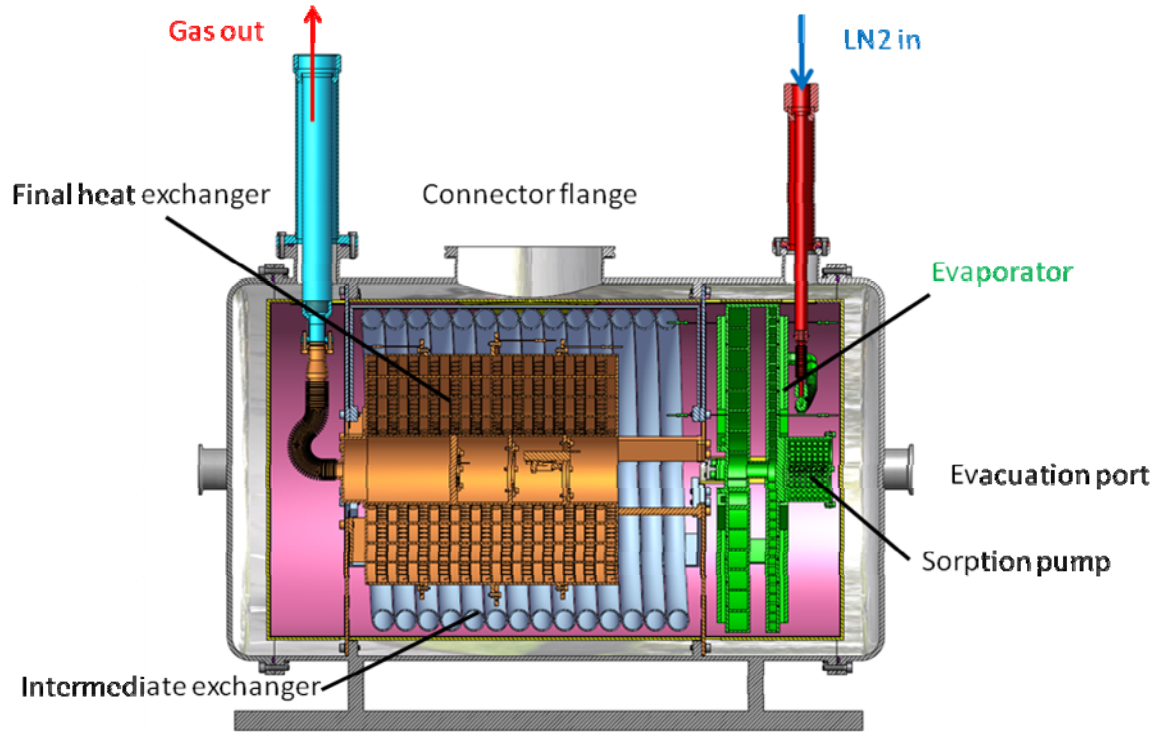Figure 3. General view of the Preparation Unit.

Figure 4. Cut view of the Preparation Unit showing the different systems inside. The Evaporator Unit makes the LN2 change to gaseous phase. The Intermediate Exchanger is composed by a coils providing additional stabilization of the gas flow. Next, the flow comes into the Final Heat Exchanger, which provides a huge exchange area with the gas. This stage provides the final step of the flow up to the working temperature.

## 4. THERMAL ANALYSES IMPLEMENTED

The analyses here presented deal with two main issues related with the thermal stability requirement. First, the temperature on the optical bench (see section 4.1) is found as a response to a sine-shaped temperature signal on the radiation shield. The input signal introduces a sort of instability in the temperature control of the radiation shield.

Secondly, some finite element analysis (FEA) models (see section 4.2) have been implemented to find the steady-state temperature distribution on the radiation shield and the optical bench.

### 4.1 Thermal stability analysis

Given a sine-shaped thermal input on the radiation shield, the thermal response on the optical bench is found. Thus, an idea of the thermal damping of the system is provided. Homogeneous temperatures on the optical bench and the radiation shield have been assumed for this transient analytical routine.

The radiation shield temperature is given according to a sine law (see Eq. (1)). The sinusoidal amplitude has been set at a conservative value of ±0.5 K, the working temperature being 140 K.

On the other hand, the response's amplitude strongly depends on the frequency of the input signal. Furthermore, the input signal's frequency is highly dependent on the masses and the specific heat of the radiation shield. Indeed, these parameters will define how long the radiation shield takes to change its temperature by a certain amount after a certain amount of energy has been provided.

As a first approach, the input signal's frequency is estimated in 2 hours. This figure is likely to be conservative from the standpoint of the control due to the relatively low mass of the shield. Note that the shorter the input period is the smaller the response's amplitude.

Both the optical bench and the radiation shield are considered to be made of aluminium. The mass of the optical bench is assumed to be 800kg approximately. The emissivity of the surfaces here involved is 0.95. These are the inner surface of the radiation shield and the outer surface of the optical bench. This high emissivity value is not convenient for a high radiative decoupling of between the radiation shield and the optical bench; nevertheless, it is necessary in order to minimize ghosts that may affect the detector.

The present routine is based on a series of time steps ($\Delta t$=30s). At each moment $i$-$1$, the value of the input signal is found according to Eq. (1), as well as the radiative heat exchange ($W_{RadSh \rightarrow OB}$) between the radiation shield and the optical bench (Eq. (2)). This power -applied upon a time step- gives the energy ($Q_{OB}$) applicable to the optical bench during the present time step (Eq. (3)). Now, the temperature of the optical bench at the moment $i$ can be found by means of the Eq. (4).

$$T_{RadSh}(t) = 140 + 0.5 \cdot \cos\left(\frac{2\pi}{7200} \cdot t\right) \tag{1}$$

$$\left(W_{RadSh \rightarrow OB}\right)_{i-1} = \frac{\sigma \cdot \left(\left(T_{RadSh}\right)_{i-1}^4 - \left(T_{OB}\right)_{i-1}^4\right)}{\left(\dfrac{1 - \varepsilon_{RadSh}}{\varepsilon_{RadSh} \cdot A_{RadSh}}\right) + \dfrac{1}{A_{RadSh} \cdot F_{RadSh \rightarrow OB}} + \left(\dfrac{1 - \varepsilon_{OB}}{\varepsilon_{OB} \cdot A_{OB}}\right)} \tag{2}$$

$$\left(Q_{OB}\right)_i = \left(W_{RadSh \rightarrow OB}\right)_{i-1} \cdot \Delta t \tag{3}$$

$$\left(T_{OB}\right)_i = \left(T_{OB}\right)_{i-1} - \frac{\left(Q_{OB}\right)_i}{m_{OB} \cdot \left(Ce\right)_{OB}} \tag{4}$$

Figure 5 shows the temperature in time both of the radiation shield and the optical bench. The response on the optical bench ranges from 140.01 K and 139.99 K during 1 day time. This fits with the goal stated in section 2, the requirement being achieved by far.
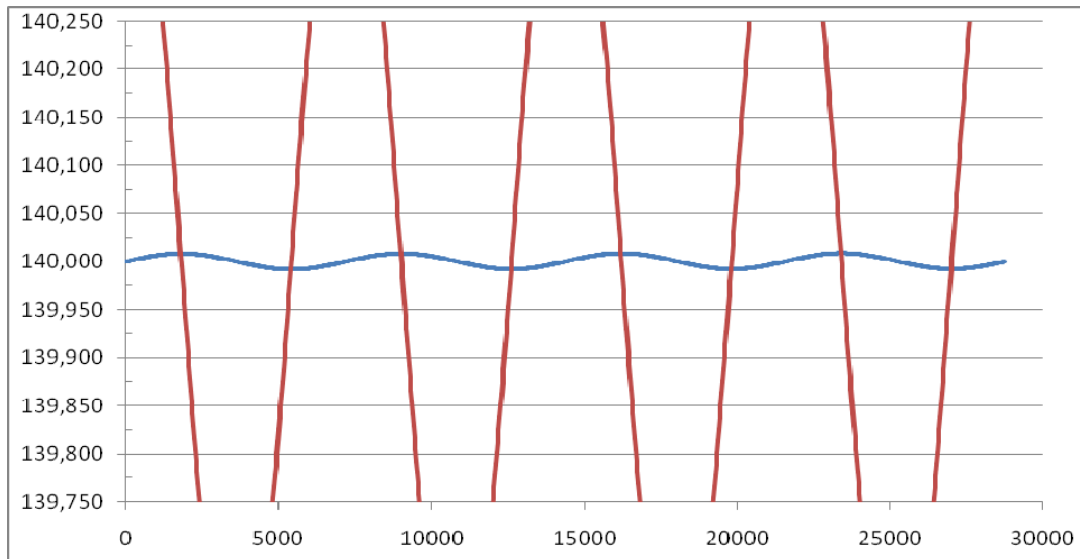


Figure 5. Graph showing the temperature (K) in time (sec) of the radiation shield (sine-shaped input signal; red colour) and the optical bench (sine-shaped temperature response; blue colour).

## 4.2 FEA steady-state analysis

The main aim of the FEA analyses here described is the temperature distribution across both the radiation shield and the optical bench in the steady-state. Thus, the following sequence has been implemented in order to provide a highly reliable model, as well as reasonable in terms of computation:

- Calculation of the radiative load to the radiation shield from the vacuum vessel (Model I): This model (see Figure 6) includes only the Vacuum Vessel and the radiation shield in order to have an easy-to-manage model in terms of computation, which means the assumption of negligible radiative exchange between radiation shield and optical bench. The latter assumption will be further checked.

  With some minor simplifications, the geometry of the radiation shield is close to the real one. For each piece of the radiation shield, the radiative load coming from the Vacuum Vessel is found (see Figure 8).

- Optimization of the position of the heat exchangers on the radiation shield for any cooling line –composed by two heat exchangers in series- to dissipate approximately the same amount of power as each other.

- Estimate of the temperature of the heat exchangers.


### 4.2.1 *The model for the calculation of the radiative load (Model I).*

Since the radiation shield is cooled down by means of several heat exchangers whose exchange area is small as compared to the area of the entire shield, a temperature distribution across the shield will be produced, the thermal gradient being not negligible. Nevertheless, deviations of few degrees with respect to 140 K will not affect the radiative load here found.

More importantly, an additional check (see Model II) has to be done with respect to the conductive losses through the legs attaching the optical bench to the Vacuum Vessel. These losses are compensated in the steady-state by radiative exchange between the radiation shield and the optical bench. Therefore, since the Model I does not include the optical bench, the conductive losses have to be low as compared to the radiative load from the Vacuum Vessel to the radiation shield. Otherwise, the optical bench should be also included in the Model I because the radiative exchange between the latter and the radiation shield would not be negligible as compared to the radiative exchange between the radiation shield and the Vacuum Vessel.

The present model is shown in Figure 6, as well as the main dimensions. Although they are not shown, both the Vacuum Vessel and the radiation shield have been modeled with covers –at the front and in the rear. The boundary conditions here introduced are the following:

- The temperature of the Vacuum Vessel is 285 K (room temperature).

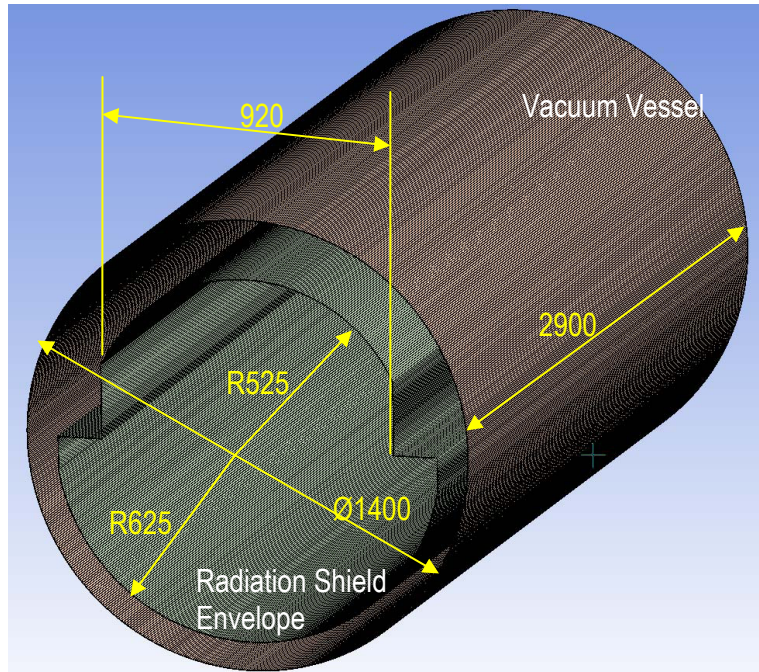- The temperature of the radiation shield is 140 K.

Figure 6. View showing the Model I, as well as the main dimensions applicable.

### 4.2.2  Optimization of the position of the heat exchangers on the radiation shield (Model II).

The model here implemented (Model II) is shown in Figure 7 and includes only the radiation shield and the optical bench. The different lines cooling the shield are composed by two heat exchangers in series, except for the covers, each of them being cooled by one heat exchanger. Therefore, the optimization of the position of the heat exchangers is done through several trials where the respective locations of both heat exchangers of each line have been changed such a way that the power dissipated through all the lines is approximately the same.

### 4.2.3  Estimate of the temperature of the heat exchangers (Model II)

Once the location of the heat exchangers has been defined, the Model II itself is run through several trials in order to estimate the temperature of the heat exchangers. For each cooling line, the boundary conditions affecting the temperature of the heat exchangers are varied in the following terms:

- The temperature of the first heat exchanger has been fixed to 135 K

- The temperature of the second heat exchanger ranges from 136 K to 140 K by increasing steps of 1 K.

The FEA model used for these trials includes the optical bench, the radiation shield and the legs attaching the optical bench to the Vacuum Vessel. The rest of boundary conditions are listed below:

- Warm end of the legs at 285 K

- Radiative load affecting to each piece of the radiation shield according to the figures found through the Model I (see Figure 8, right).
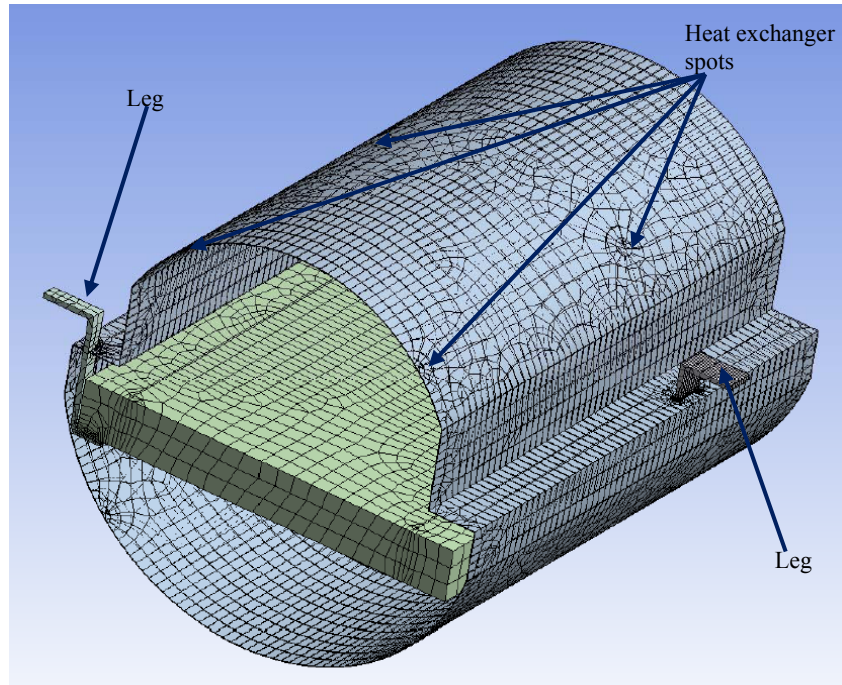
Figure 7. View showing the Model II as meshed, as well as the main dimensions applicable. The model is half the length of the real one.

### 4.2.4 Results obtained

From Model I the resulting radiative load from the Vacuum Vessel to the radiation shield is about 12.44W. Figure 8 shows the net heat flows in the steady-state within the system including the Vacuum Vessel, the radiation shield and the optical bench. The same figure also shows the heat flows dissipated through the heat exchangers attached to the main body of radiation shield. The heat exchanger attached to each cover drains about 0.96W. The total power dissipated through the heat exchangers is 13.4W due to the additional losses through the legs attaching the optical bench to the Vacuum Vessel (0.96W).

Note that the same legs supporting the optical bench also hold the radiation shield. From the value above mentioned, 0.79W come into the radiation shield while only 0.17W come into the optical bench. The only way to dissipate the latter value is by radiation from the optical bench to the radiation shield. This confirms the assumption made for the Model I, where the radiative exchange between the optical bench and the radiation shield was considered negligible.

From Model II applied to the step 4.2.3, it was found that the temperature gap between both heat exchangers of each line cannot be larger than 3 K; otherwise, the second heat exchanger scarcely works. Since the temperature of the first heat exchanger was fixed to 135 K, the second one cannot be warmer than 138 K. As these temperatures provide a quite reasonable, conservative scenario, they have been introduced in the Model II, thus providing the conditions for obtaining the temperature distribution of both the radiation shield and the optical bench.

Figure 9 shows the temperature distribution across the radiation shield. The spots of the cool heat exchangers are on the upper radiation shield while the warm spots are on the lower radiation shield. The temperature gradient of the radiation shield ranges from 134 K to 138.6 K. On the other hand, Figure 10 shows the temperature distribution across the optical bench, the resulting gradient ranging inside a narrow band of 0.02 K around 137.8 K. This confirms, therefore, that the present concept for the cooling system of the NIR channel of the CARMENES instrument provides very smooth gradients on the optical bench.
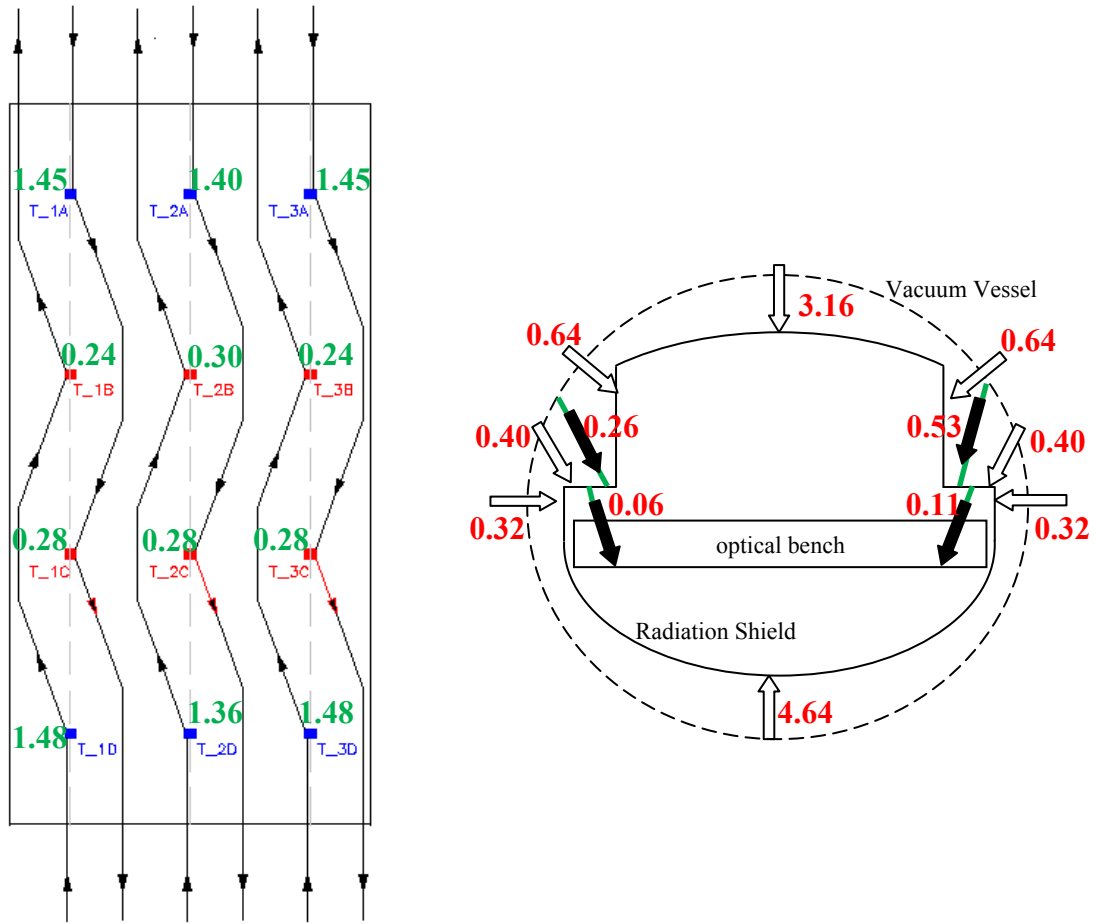
Figure 8. *Right*: Layout showing the steady-state net heat flows (in watts) within the system composed by the optical bench, the radiation shield and the Vacuum Vessel. Note that the covers of the radiation shield are not shown. The radiative load to each cover coming from the Vacuum Vessel is 0.96W. The conductive losses are marked by black arrows while white arrows mark net radiative flows. *Left*: The different heat flows drained through the heat exchangers on the main body of the radiation shield. For each line with two heat exchangers in series, the blue is the cool one while the red one is the warm one. For better understanding, this layout shows the radiation shield in unfolded mode.
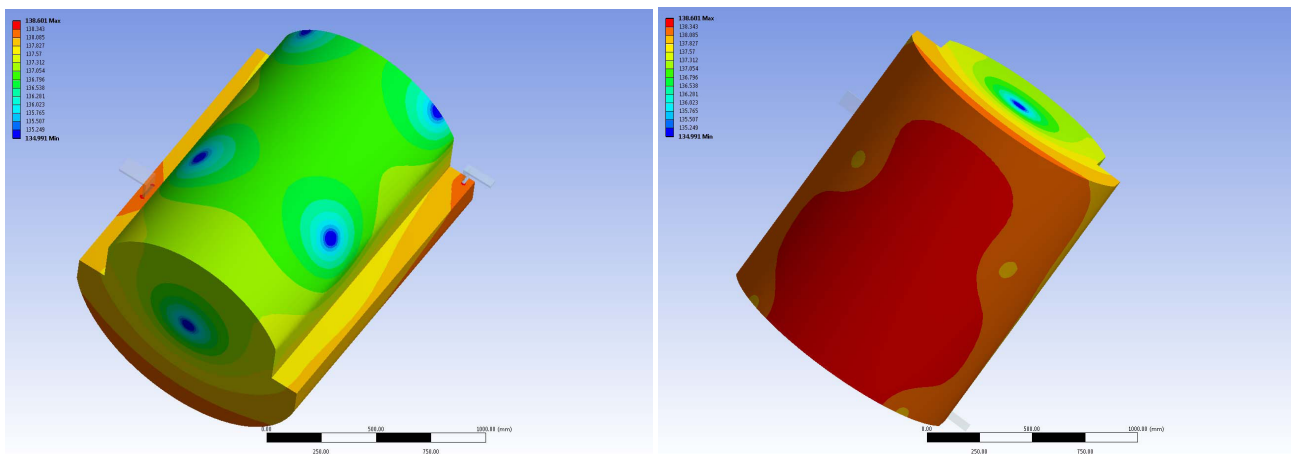


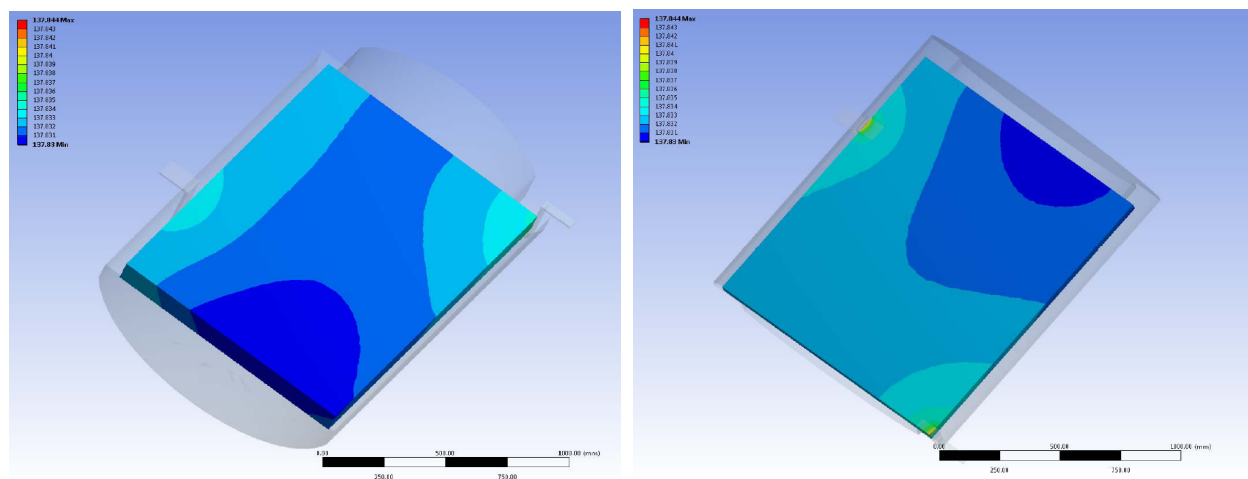Figure 9.Views showing the temperature distribution across the radiation shield.

Figure 10. Views showing the temperature distribution across the optical bench.

# 5. CONCLUSIONS AND FURTHER TASKS

Models here presented confirm that the concept for the cooling system of the CARMENES NIR channel is going to provide very smooth temperature gradients on the optical bench. Furthermore, the optical bench will be highly stabilized by means of radiative heat exchange with the radiation shield, the thermal stability requirement being ensured and its goal being likely achieved.

Presently, tasks are ongoing to manufacture the Preparation Unit and make the first tests in order to know the main parameters of the system. This knowledge of the system will be used to cross-check the current FEA model. Indeed, an analytical model is being implemented to find the temperature of the nitrogen gas flow from given temperatures on the heat exchangers, thus the power evacuated by the gas matching the power dissipated through the heat exchangers.

Due to the key role of the cooling system, the AIV (assembly, integration and verification) phase for the cooling system inside the instrument is scheduled as one of the earliest tasks, even if that runs in parallel to the opto-mechanical assembly and integration in warm conditions.

# REFERENCES

[1] Becerril, S., "Comprehensive transient-state study for CARMENES NIR high-thermal stability", Proc. SPIE 7735, 77352S-1 to 77352S-13 (2010).
[2] Lizon, J.L., "Liquid nitrogen pre-cooling of large infrared instrument at ESO", Proc. SPIE 7739, 77393F-1 to 77393F-6 (2010).
[3] Lizon, J.L., Accardo, M., "LN2 continuous Flow Cryostats, a compact vibration free cooling system for single to multiple detector systems", Proc. SPIE 7739, 77393E-1 to 77393E-7 (2010).
[4] Vitali, F., Lizon, J.L., Ihle, G. et al., "The REMIR Cryogenics Restyling", Proc. SPIE 6269, 626954-1 to 626954-11 (2006)
[5] Roelfsema, R., Albers P., Lizon, J.L. et al., "X-Shooter Near Infra Red Spectrograph Cryogenic Design", Proc. SPIE 7017, 701717-1 to 701717-12 (2008).
[6] Siegel, R. and Howell, J., [Thermal radiation heat transfer], Taylor&Francis, New York, 207-250 (4th ed., 2002)
[7] Modest, M. F., [Radiative heat transfer], McGraw-Hill, Massachussets, 131-190 (2nd ed., 2003).